analytical chemistry

Article

pubs.acs.org/ac

Enhancement Effect of a Variable Topology of a Membrane-Tethered Anti-Poly(ethylene glycol) Antibody on the Sensitivity for Quantifying PEG and PEGylated Molecules

Wen-Wei Lin,[†,○] Yi-An Cheng,[‡] Chien-Han Kao,[‡] Steve R. Roffler,[¶] Yu-Chi Lee,[§] Bing-Mae Chen,[¶] Yuan-Chin Hsieh,[‡,○] I-Ju Chen,[‡] Bo-Cheng Huang,[†] Yeng-Tseng Wang,[∥,○] Yi-Ching Tung,[⊥] Ming-Yii Huang,[#,○] Fang-Ming Chen,[*,▽] and Tian-Lu Cheng[*,†,‡,§,○,◆]

[†]Institute of Biomedical Sciences, National Sun Yat-sen University, Kaohsiung, Taiwan

[‡]Graduate Institute of Medicine, College of Medicine, [§]Department of Biomedical Science and Environmental Biology, [∥]Department of Biochemistry, [⊥]Department of Public Health and Environmental Medicine, College of Medicine, [#]Department of Radiation Oncology, Cancer Center, Kaohsiung Medical University Hospital, [▽]Department of Surgery, Faculty of Medicine, College of Medicine, [○]Center for Biomarkers and Biotech Drugs, and [◆]Department of Medical Research, Kaohsiung Medical University Hospital, Kaohsiung Medical University, Kaohsiung, Taiwan

[¶]Institute of Biomedical Sciences, Academia Sinica, Taipei, Taiwan

ABSTRACT: Sensitive quantification of the pharmacokinetics of poly(ethylene glycol) (PEG) and PEGylated molecules is critical for PEGylated drug development. Here, we developed a sensitive sandwich enzyme-linked immunosorbent assay (ELISA) for PEG by tethering an anti-PEG antibody (AGP3) via tethers with different dimensions on the surface of 293T cells (293T/S-αPEG, short-type cells; 293T/L-αPEG, long-type cells; 293T/SL-αPEG, hybrid-type cells) to improve the binding capacity and detection limit for free PEG and PEGylated molecules. The binding capacity of hybrid-type cells for PEG-like molecules (CH_3-PEG_{5K}-FITC (FITC = fluorescein isothiocyanate) and eight-arm PEG_{20K}-FITC) was at least 10−80-fold greater than that of 293T cells expressing anti-PEG antibodies with uniform tether lengths. The detection limit of free PEG (OH-PEG_{3K}-NH_2 and CH_3-PEG_{5K}-NH_2) and PEG-like molecule (CH_3-PEG_{5K}-FITC, CH_3-PEG_{5K}-SHPP, and CH_3-PEG_{5K}-NIR797) was14−137 ng mL^{-1} in the hybrid-type cell-based sandwich ELISA. 293T/SL-αPEG cells also had significantly higher sensitivity for quantification of a PEGylated protein (PegIntron) and multiarm PEG macromolecules (eight-arm PEG_{20K}-NH_2 and eight-arm PEG_{40K}-NH_2) at 3.2, 16, and 16 ng mL^{-1}, respectively. Additionally, the overall binding capacity of 293T/SL-αPEG cells for PEGylated macromolecules was higher than that of 293T/S-αPEG or 293T/L-αPEG cells. Anchoring anti-PEG antibodies on cells via variable-length tethers for cell-based sandwich ELISA, therefore, provides a sensitive, high-capacity method for quantifying free PEG and PEGylated molecules.

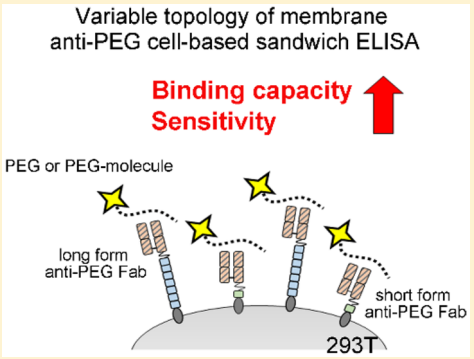

Poly(ethylene glycol) (PEG) is a highly water-soluble, nonimmunogenic, and biocompatible polymer that is approved by the Food and Drug Administration (FDA) for human use in the clinic.[1] Chemical modification of PEG can improve the hydrophilicity, reduce the immunogenicity, decrease the systemic toxicity, and prolong the serum half-life of both small molecules and biotherapeutic drugs.[1] For example, Rowinsky and colleagues showed that conjugating camptothecin (CPT) to a chemically modified PEG molecule increases the aqueous solubility, serum half-life (3.5 fold), and overall feasibility of CPT from a pharmaceutical standpoint in cancer therapy.[2,3] Zhao et al. reported the preparation of a multiarm PEG backbone linked to four SN38 molecules (PEG-SN38) with high drug loading and significantly improved water solubility (400−1000-fold increase) for treatment of advanced colorectal cancer.[4] Greenwald and colleagues also demonstrated a prodrug strategy for paclitaxel employing PEG as a solubilizing agent as an alternative method to improve water solubility and effectiveness in vivo in comparison with traditional cremophor EL formulations.[5] Additionally, PEG is also widely attached to peptides,[6] proteins,[7−11] micelles,[12−14] liposomes,[15−17] and nanoparticles[18−20] to improve in vivo biological efficacy. The efficient analysis of the pharmacokinetics of free PEG and PEGylated molecules is an important subject with increasing numbers of such compounds under development.

Development of a simple, accurate, and sensitive method to quantify free PEG and PEGylated molecular drugs in complex biological samples is important for drug development and clinical trials. However, traditional anti-PEG antibody-based

Received: February 27, 2017
Accepted: May 9, 2017
Published: May 9, 2017

DOI: 10.1021/acs.analchem.7b00730
Anal. Chem. 2017, 89, 6082−6090

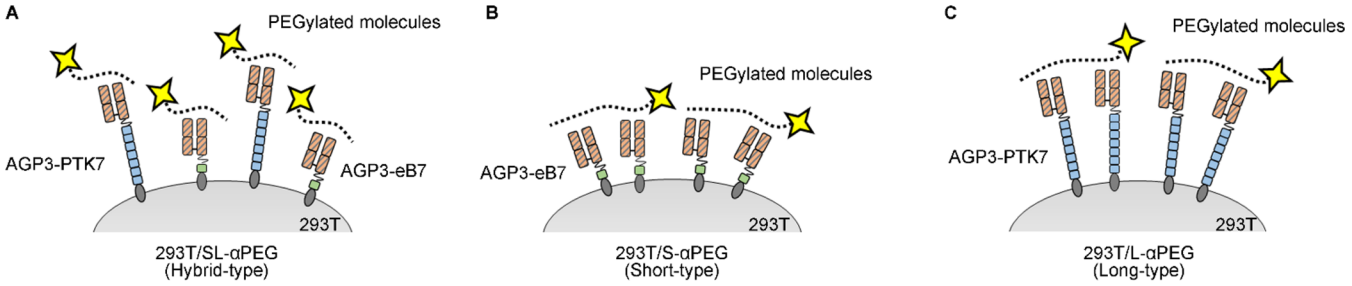

Figure 1. Topology of membrane-anchored anti-PEG antibodies, which may affect the binding capacity and detection limit of PEGylated molecules. AGP3 anti-PEG Fab was expressed on 293T cells via (A) both short and long tethers (293T/SL-αPEG cells), (B) short tethers (293T/S-αPEG cells), or (C) long tethers (293T/L-αPEG cells). Serially diluted PEG molecules were detected by cell-based sandwich ELISA in combination with biotinylated anti-PEG antibodies (AGP4) and horseradish peroxidase (HRP)-conjugated streptavidin.

enzyme-linked immunosorbent assay (ELISA) is insensitive for quantification of small PEG molecules.[21] Anti-PEG cell-based sandwich ELISA can improve the sensitivity of PEG detection by displaying unidirectional orientation of surface anti-PEG antibodies, but the detection limit remains relatively poor for PEG molecules smaller than 10000 Da because of fewer epitopes for anti-PEG antibody binding.[22] Increasing the contact area between PEG molecules and binding antibodies may improve the quantitative sensitivity of anti-PEG cell-based sandwich ELISA. Jain and colleagues suggested that modifying the poly(2-(methacryloyloxy)ethyl succinate) (poly(MES)) brushes on porous nylon membranes can increase the surface binding area and facilitate the efficacy of lysozyme purification. The binding capacity of lysozyme from chicken egg white was enhanced 2−4-fold in poly(MES)-modified nylon membranes as compared with commercial ion-exchange membranes.[23] Barua et al. showed that the surface area of nanoparticles affects the specificity and capacity of modified antibodies. Rod-shaped nanoparticles provide higher surface area per unit volume compared with sphere-shaped nanoparticles and can therefore absorb higher amounts of trastuzumab antibody. The trastuzumab-coated rods exhibited greater inhibitory ability of BT-474 breast cancer cell growth in vitro as compared with soluble forms of the antibody.[24] On the basis of these reports, we hypothesized that altering the topology of anti-PEG antibodies on the surface of cells might enhance the contact area between PEG and anti-PEG antibodies and further improve the assay sensitivity for quantification of PEG molecules.

In this study, we investigated the effect of the tether dimensions of a membrane-anchored anti-PEG antibody on the quantification sensitivity of free PEG and PEGylated molecules. The Fab domain of the AGP3 anti-PEG antibody was expressed on the surface of 293T cells via short, long, or mixed short and long tethers (Figure 1). We analyzed the capacity of the cells to bind PEG_{5K}-FITC (FITC = fluorescein isothiocyanate) and eight-arm PEG_{20K}-FITC and measured their detection limit in cell-based sandwich ELISA for free PEG (OH-PEG_{3K}-NH_2 and CH_3-PEG_{5K}-NH_2), PEG-like molecules (CH_3-PEG_{5K}-FITC, CH_3-PEG_{5K}-SHPP, and CH_3-PEG_{5K}-NIR797), a PEGylated macromolecule (CH_3-PEG_{12K}-IFNα-2b, PegIntron), and multi-arm PEG molecules (eight-arm PEG_{20K}-NH_2 and eight-arm PEG_{40K}-NH_2). Our data suggest that expressing anti-PEG antibodies on cells via both short and long tethers may provide a sensitive tool for quantification and pharmacokinetic studies of free PEG and PEGylated molecules.

EXPERIMENTAL SECTION

Cells and Reagents. 293T human embryonic kidney epithelial cells (American Type Culture Collection, Manassas, VA) were cultured in Dulbecco's modified Eagle's medium (DMEM; Sigma-Aldrich, St. Louis, MO) containing 10% (v/v) heat-inactivated bovine calf serum (BCS; Thermo, Waltham, MA) and 100 units mL^{-1} penicillin and streptomycin (Invitrogen, Calsbad, CA) at 37 °C in a humidified atmosphere of 5% (v/v) CO_2. PegIntron was from Roche (Nutley, NJ). Skim milk was purchased from BD Difco (Franklin Lakes, NJ). OH-PEG_{3K}-NH_2 (average M_n = 3000), CH_3-PEG_{5K}-NH_2 (average M_n = 5000), eight-arm PEG_{20K}-NH_2 (average M_n = 20000), and eight-arm PEG_{40K}-NH_2 (average M_n = 40000) were purchased from Fluka Chemie (Buchs, Switzerland). Poly(lactic acid) (PLA; $M_w \approx 60000$) and polycaprolactone (PCL; $M_w \approx 14000$) were purchased from Sigma-Aldrich. 2,2′-Azinobis[3-ethylbenzothiazoline-6-sulfonic acid] (ABTS) and 30% hydrogen peroxide were from Sigma-Aldrich. Horseradish peroxidase (HRP)-conjugated streptavidin was from Jackson Immunoresearch Laboratories (West Grove, PA). Eight-arm PEG_{20K}-FITC, CH_3-PEG_{5K}-FITC, CH_3-PEG_{5K}-3-(4-hydroxyphenyl)propionic acid *N*-hydroxysuccinimide ester (SHPP), and CH_3-PEG_{5K}-near-infrared 797 (NIR797) were synthesized as previously described.[25]

Plasmid Construction. The V_L-C_κ and V_H-C_{H1} domains of the anti-PEG antibody were cloned from cDNA prepared from the AGP3 hybridoma following a previously described method.[26,27] Primers used in the cloning of V_L-C_κ and V_H-C_{H1} were as follows: V_L-C_κ sense, 5′-tgctggggcccagccggccg-atattgtgttgacgcaggct-3′; V_L-C_κ antisense, 5′-ccgctcgagacactc-attcctgttgaagct-3′; V_H-C_{H1} sense, 5′-gaagatctgaagtgcagctggtgga-gtct-3′; V_H-C_{H1} antisense, 5′-caggtcgacagctggaatgggcacatgcag-3′. The light- and heavy-chain sequences, joined by a furin-2A protease cleavage site,[28] were subcloned into two lentiviral vectors, pLKO_AS3-eB7 and pLKO_AS3-PTK7-eB7, by use of *Hind*III and *Sal*I restriction sites. The expression vectors, pLKO_AS3-AGP3-eB7 and pLKO_AS3-AGP3-PTK7-eB7, encode an anti-PEG Fab fused to the immunoglobulin C2-type extracellular transmembrane−cytosolic domains of the mouse B7-1 antigen (eB7) or immunoglobulin C2-type domain of the tyrosine protein kinase 7 (PTK7)-eB7 (Figure 2A).

Generation of Short-, Long- and Hybrid-Tethered Anti-PEG-Expressing Cells by Lentiviral Transduction. Pseudotyped lentiviruses were generated by cotransfecting pLKO_AS3-AGP3-eB7 or pLKO_AS3-AGP3-PTK7 with pCMVΔR8.91 or pMD.G (Academia Sinica, Taipei, Taiwan), respectively, in 293T cells by PureFection (System Biosciences, Palo Alto, CA). Two days after transfection, the culture

DOI: 10.1021/acs.analchem.7b00730
Anal. Chem. 2017, 89, 6082−6090

medium was filtered, mixed with 8 μg mL^{-1} Polybrene (Sigma-Aldrich), and added to 293T cells. Following lentiviral transduction, the cells were selected in 2 μg mL^{-1} puromycin- or 100 μg mL^{-1} hygromycin-containing medium and sorted on a FACS Cantor (Beckman Coulter, Brea, CA) to generate anti-PEG cells that stably expressed approximately equal levels of short-, long-, or hybrid-tethered anti-PEG antibodies on their surface.

Western Blot Analysis of the Anti-PEG-Expressing Cells. 293T/S-αPEG (short-type), 293T/L-αPEG (long-type), and 293T/SL-αPEG (hybrid-type) cells (2×10^5) were collected and boiled for 5 min in nonreducing sample buffer. The samples were electrophoresed in an 8% sodium dodecyl sulfate (SDS)−polyacrylamide gel under nonreducing conditions and then transferred onto nitrocellulose paper (Merck Millipore, Billerica, MA). After blocking with 5% skim milk, the membrane was incubated with either 0.4 μg/mL HRP-conjugated goat antimouse IgG F(ab′)$_2$ antibody (Jackson Immunoresearch Laboratories) or mouse antihuman β-actin antibody (Novus Biologicals, Littleton, CO). After being washed four times with PBST (PBS containing 0.05% Tween 20) and once with PBS, the membrane stained with anti-β-actin antibody was then incubated with HRP-conjugated goat antimouse IgG F(ab′)$_2$ antibody. After extensive washing, the blots were visualized by enhanced chemiluminescence detection according to the manufacturer's instructions (Merck Millipore). The bands of anti-PEG Fab and β-actin were quantified by densitometry with the Gel-Pro Analyzer 4.0 software.

Fluorescence-Activated Cell Sorting Analysis of the Anti-PEG-Expressing Cells. Surface expression of the anti-PEG Fab was measured by staining the cells with 3.75 μg mL^{-1} FITC-conjugated goat antimouse IgG F(ab′)$_2$ (Jackson Immunoresearch Laboratories) in PBS containing 0.05% (w/v) bovine serum albumin (BSA) on ice. The PEG binding activity of membrane-tethered anti-PEG Fab was determined by incubating the cells with 10 μg mL^{-1} CH$_3$-PEG$_{5K}$-FITC or 250 ng mL^{-1} eight-arm PEG$_{20K}$-FITC in PBS containing 0.05% (w/v) BSA on ice. After removal of unbound antibodies, CH$_3$-PEG$_{5K}$-FITC, or eight-arm PEG$_{20K}$-FITC by extensive washing in cold PBS containing 0.05% (w/v) BSA, the surface fluorescence of the viable cells was measured on a FACScan flow cytometer (BD Biosciences, San Jose, CA), and the fluorescence intensities were analyzed with FlowJo7.6.1 software (Tree Star, San Carlos, CA). The binding capacities of hybrid-type (293T/SL-αPEG), short-type (293T/S-αPEG), and long-type (293T/L-αPEG) cells for free PEG and PEGylated molecules were determined by incubating the cells with serially diluted CH$_3$-PEG$_{5K}$-FITC probe (10, 3.3, 1.1, 0.4, 0.12, and 0.04 μg mL^{-1}) or eight-arm PEG$_{20K}$-FITC probe (2500, 833, 278, 93, 31, and 10.3 ng mL^{-1}) in PBS containing 0.05% (w/v) BSA on ice. After removal of unbound probes by extensive washing in cold PBS containing 0.05% (w/v) BSA, the surface fluorescence of the viable cells was measured on a FACScan flow cytometer.

Anti-PEG Cell-Based Sandwich ELISA. In all sandwich ELISA experiments, PBS containing 2% (w/v) skim milk was used as the sample dilution buffer and PBS was used as the wash buffer. The short-, long-, or hybrid-type anti-PEG cells (2×10^5 cells per well) were seeded overnight in 96-well plates (Nalge Nunc International, Roskilde, Denmark) coated with 50 μg mL^{-1} poly-D-lysine (Corning, New York) in culture medium. After extensive washing, the cells were fixed with 2% (w/v) paraformaldehyde for 5 min at room temperature (rt). The fixed reaction was stopped by 0.1 M glycine for 30 min at rt. In our previous study, there was no significant difference in anti-PEG antibody binding in fixed and nonfixed anti-PEG (AGP3)-expressing cells.[29] The plates were blocked with 5% (w/v) skim milk in PBS for 2 h at 37 °C. Graded concentrations of PLA, PCL, OH-PEG$_{3K}$-NH$_2$, CH$_3$-PEG$_{5K}$-NH$_2$, CH$_3$-PEG$_{5K}$-FITC, CH$_3$-PEG$_{5K}$-SHPP, CH$_3$-PEG$_{5K}$-NIR797, PEGIntron (Schering-Plough, Kenilworth, NJ), eight-arm PEG$_{20K}$-NH$_2$, or eight-arm PEG$_{40K}$-NH$_2$ were added to the wells (50 μL per well) at rt for 1 h. After washing, the cells were sequentially incubated with biotinylated AGP4 (0.25 μg per well) and HRP-conjugated streptavidin (HRP−streptavidin, 50 ng per well). The plates were washed with PBS, and the bound peroxidase activity was measured by adding 150 μL of ABTS solution [0.4 mg mL^{-1}, 2,2′-azinobis[3-ethylbenzothiazoline-6-sulfonic acid] (Sigma-Aldrich), 0.01% (v/v) H_2O_2, and 100 mM phosphate−citrate, pH 4.0] per well for 1 h at rt. Color development was measured at 405 nm on a microplate reader (Molecular Devices, Menlo Park, CA).

Modeling the Structures and Calculating the Length of Short-Type (AGP3-eB7) and Long-Type (AGP3-PTK7) Anti-PEG Fab. The three-dimensional structure of short-type (AGP3-eB7) and long-type (AGP3-PTK7) anti-PEG Fab was modeled by SWISS-Modeling (https://swissmodel.expasy.org/), which is a fully automated protein structure homology-modeling server. The Ig-like C2 domain of eB7 (residues 143−246) was built using B7-1 (PDB code 1DR9, 58.7% sequence identity) as a template. The 247−268 transmembrane region and the 269−306 cytoplasmic domain of eB7 were built using CD4 (PDB code 2KLU, 23.33% identity). The first through sixth N-terminal Ig-like C2 domains (residues 31−586) and the seventh domain (residues 578−680) of PTK7 were built using titin (PDB code 3B43, 23.53% identity) and Sidekick-1 (PDB code 5K6W, 38.24% identity). The structure of AGP3 anti-PEG Fab was modeled by Discovery Studio (DS) software. The modeled fragment structures were merged to generate the structural model of AGP3-eB7 and AGP3-PTK7. The structures were then visualized and the molecular length of each domain was calculated by PyMol software (DeLano Scientific).

Statistical Analysis. All the readings were background-adjusted by subtracting the absorbance of a blank control in the ELISA procedures. The detection limit of the ELISA experiments was determined by using an independent t test to compare the statistical significance of the differences between the controls and samples (free PEG and PEGylated molecules). Data were considered significant at a P value of less than 0.05.

RESULTS AND DISCUSSION

Characterization of Short-, Long-, or Hybrid-Tethered Anti-PEG Antibody-Expressing 293T Cells. To increase antigen−antibody interactions on the cell surface, we expressed anti-PEG antibodies (AGP3) with different lengths of tethers on the membrane of 293T cells. We selected the immunoglobulin-like (Ig-like) C2-type extracellular transmembrane−cytosolic domains of the mouse B7−1 antigen (eB7) as a short tether and the extracellular region of the tyrosine protein kinase 7 (PTK7), which contains seven Ig-like C2-type domains, as a long tether. We constructed two lentiviral vectors, pLKO_AS3-AGP3-eB7 and pLKO_AS3-AGP3-PTK7, to

DOI: 10.1021/acs.analchem.7b00730
Anal. Chem. 2017, 89, 6082−6090

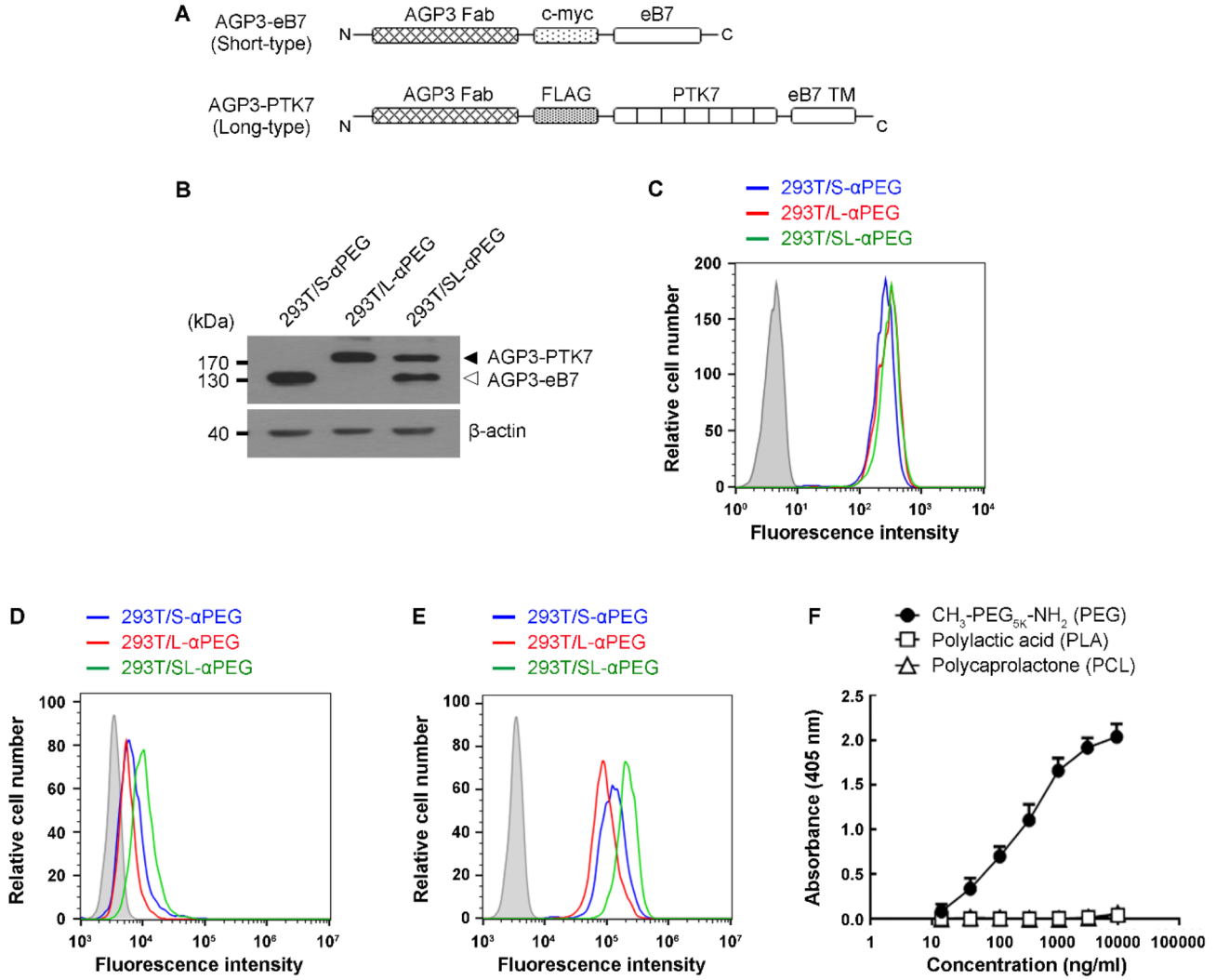

Figure 2. Membrane expression of functional hybrid-, short-, or long-type anti-PEG antibodies on 293T cells. 293T/SL-*α*PEG, 293T/S-*α*PEG, and 293T/L-*α*PEG cells were generated that stably express AGP3-eB7 (short chain) or AGP3-PTK7 (long chain) on 293T cells individually or together. (A) Schematic of the short-chain anti-PEG antibody including (from the N to C terminus) the anti-PEG Fab (AGP3) fragment (composed of a light chain, furin-2A, and a heavy chain), a c-myc epitope, and the Ig-like C2-type extracellular transmembrane (TM)−cytosolic domain of the murine B7-1 antigen (eB7). The long chain of the anti-PEG antibody includes (from the N to C terminus) the Fab fragment of AGP3, a FLAG tag, an extracellular domain (containing seven Ig-like C2-type domains) of human tyrosine protein kinase 7 (PTK7), and the TM and cytoplasmic domains of eB7. (B) Western blotting analysis of protein expression of three types of anchored anti-PEG Fab on the cell surface: lane 1, 293T/S-*α*PEG; lane 2, 293T/L-*α*PEG; lane 3, 293T/SL-*α*PEG. The black arrow indicates the long type of membrane anti-PEG Fab (AGP3-PEK7). The white arrow indicates the short type of membrane anti-PEG Fab (AGP3-eB7). 293T/SL-*α*PEG (green lines), 293T/S-*α*PEG (blue lines), and 293T/L-*α*PEG (red lines) were also analyzed by flow cytometry using (C) a specific antibody to the mouse IgG $F(ab')_2$ to assess surface expression or staining with (D) CH_3-PEG_{5K}-FITC or (E) eight-arm PEG_{20K}-FITC to assess the PEG-binding activity of all three types of cells. The shaded area on the graphs shows mock staining with PBS containing 0.05% (w/v) BSA. (F) Measurement of the concentration of CH_3-PEG_{5K}-NH_2 (PEG) (●), poly(lactic acid) (PLA) (□), and poly(caprolactone) (PCL) (△) via sandwich ELISA with 293T/SL-*α*PEG cells as the capture reagents and the biotinylated anti-PEG antibody (AGP4) as the detection antibody. The mean absorbance values (405 nm) of triplicate determinations are shown. The bars indicate the SD.

directly express and anchor the Fab fragment of AGP3 (anti-PEG antibody) on the cells. In these two constructs, the AGP3 light (V_L-C_κ) and heavy (V_H-C_{H1}) chains are separated by a furin cleavage site and 2A peptide (Figure 2A), which allows antibody expression from a single open reading frame.[28] Human embryonic kidney epithelial 293T cells were infected with recombinant lentivirus containing pLKO_AS3-AGP3-eB7 or pLKO_AS3-AGP3-PTK7 plasmid individually or in combination to obtain 293T/SL-*α*PEG (hybrid-type), 293T/S-*α*PEG (short-type), and 293T/L-*α*PEG (long-type) cells.

The cell lysate of each type of cell was separated by SDS−polyacrylamide gel electrophoresis (PAGE) under nonreducing conditions and analyzed by Western blotting using a mouse $F(ab')_2$ domain specific antibody to confirm the expression of AGP3-eB7 and AGP3-PTK7. Figure 2B shows that AGP3-eB7 and AGP3-PTK7 were detected with apparent molecular weights of approximately 106400 and 197600, respectively, consistent with their expected molecular weights. The ratio of anti-PEG Fab to *β*-actin in 293T/S-*α*PEG, 293T/L-*α*PEG, and 293T/SL-*α*PEG cells approached 1, indicating that the expression levels of anti-PEG Fab in each type of cell were similar. The membrane expression and function of the anti-PEG Fab on 293T/S-*α*PEG, 293T/L-*α*PEG, and 293T/SL-*α*PEG cells was confirmed by flow cytometry after the cells

DOI: 10.1021/acs.analchem.7b00730
Anal. Chem. 2017, 89, 6082−6090

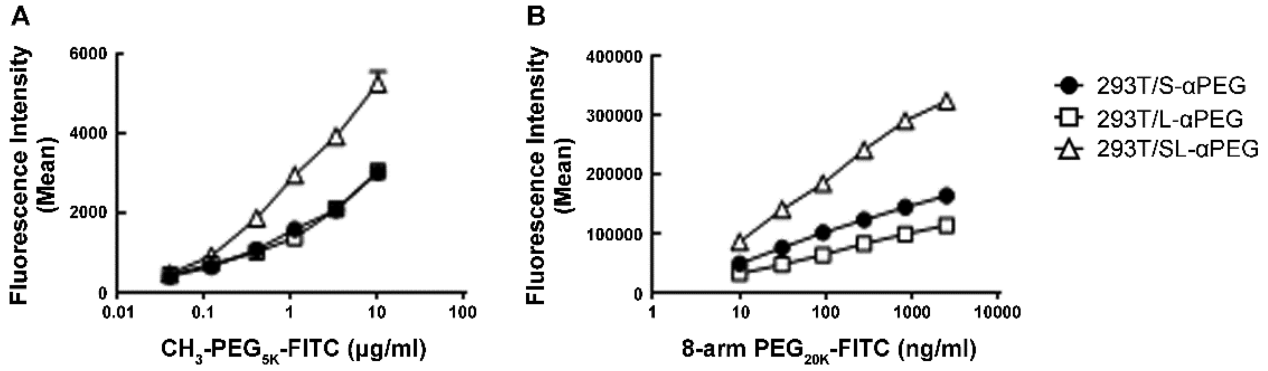

Figure 3. PEG binding capacity on hybrid-, short-, and long-type anti-PEG antibody-expressing 293T cells. Graded concentrations of (A) CH_3-PEG_{5K}-FITC or (B) eight-arm PEG_{20K}-NH_2 were added to suspended 293T/SL-*α*PEG (△), 293T/S-*α*PEG (●), and 293T/L-*α*PEG (□) cells on ice for 45 min. The fluorescence signal was detected by flow cytometry. The mean fluorescence intensities of triplicate determinations are shown. The bars indicate the SD.

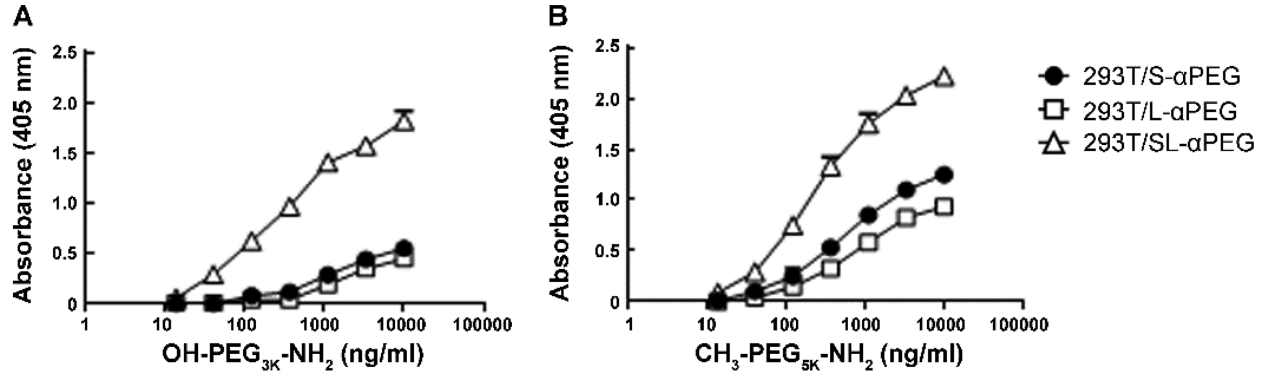

Figure 4. Quantitative cell-based ELISA for free PEG molecules. Sandwich ELISAs with 293T/SL-*α*PEG (△), 293T/S-*α*PEG (●), and 293T/L-*α*PEG (□) cells as the capture reagents and the biotinylated anti-PEG antibody (AGP4) as the detection antibody were used to measure the concentration of (A) OH-PEG_{3K}-NH_2 or (B) CH_3-PEG_{5K}-NH_2. The mean absorbance values (405 nm) of triplicate determinations are shown. The bars indicate the SD.

were directly stained with FITC-conjugated antimouse $F(ab')_2$ antibodies, CH_3-PEG_{5K}-FITC probe, or eight-arm PEG_{20K}-FITC probe to detect functional antibody binding. Figure 2C shows that AGP3-eB7, AGP3-PTK7, and AGP3-eB7 plus AGP3-PTK7 Fab fragments were expressed at similar levels on 293T/S-*α*PEG, 293T/L-*α*PEG, and 293T/SL-*α*PEG cells, respectively. All anti-PEG Fabs expressed on cells specifically bound CH_3-PEG_{5K}-FITC probe (Figure 2D) and eight-arm PEG-FITC probe (Figure 2E), indicating that surface-displayed anti-PEG Fab maintained PEG binding activity.

To analyze the cross-reactivity of anti-PEG antibody-expressing 293T cells, we coated 293T/SL-*α*PEG cells in 96-well plates, followed by addition of serial dilutions of CH_3-PEG_{5K}-NH_2 (PEG; $M_w \approx 5000$), poly(lactic acid) (PLA; $M_w \approx 60000$), and polycaprolactone (PCL; $M_w \approx 14000$). PLA and PCL polymers possess structures similar to that of PEG and also have been approved by the FDA for specific applications in humans, such as for drug delivery.[30,31] Captured molecules were quantified by sequential addition of biotinylated AGP4 anti-PEG antibody, HRP-conjugated streptavidin, and ABTS substrate. Figure 2F shows that anti-PEG Fabs expressed on cells can specifically bind to PEG in a dose-dependent manner but not PLA or PCL polymers. These results indicate that we have successfully established short-, long-, or hybrid-tethered anti-PEG antibody-expressing 293T cells, which can specifically capture PEG molecules with minimal cross-reactivity against other polymers.

Binding Capacity of PEGylated Molecules on Short-, Long-, or Hybrid-Tethered Anti-PEG Antibody-Expressing 293T Cells. To investigate whether the antibody topology can enhance the antigen binding capacity of cells, we measured the binding of small and multiarm PEG-like molecules to 293T/SL-*α*PEG (hybrid-type), 293T/S-*α*PEG (short-type), and 293T/L-*α*PEG (long-type) cells by directly staining each type of cell with serial dilutions of CH_3-PEG_{5K}-FITC or eight-arm PEG_{20K}-FITC and then detecting the fluorescence signal by flow cytometry. Figure 3 shows that the hybrid-type cells (293T/SL-*α*PEG) produced a higher fluorescence intensity of CH_3-PEG_{5K}-FITC (Figure 3A) and eight-arm PEG_{20K}-FITC (Figure 3B) compared with short-type (293T/S-*α*PEG) and long-type (293T/L-*α*PEG) cells, indicating that hybrid-type cells have at least 10-fold and 80-fold enhanced binding capacity of CH_3-PEG_{5K}-FITC and eight-arm PEG_{20K}-FITC, respectively, in comparison with uniform-length cells (293T/S-*α*PEG and 293T/L-*α*PEG). This result suggests that the variable topology created by short and long tethers may increase the contact with PEG and improve binding to small and multiarm PEG-like molecules.

Quantification of Free PEG and PEG-like Molecules by Anti-PEG Cell-Based Sandwich ELISA. To investigate the influence of the antibody topology on the assay sensitivity in a cell-based sandwich ELISA, we coated 293T/SL-*α*PEG, 293T/S-*α*PEG, and 293T/L-*α*PEG cells on 96-well plates followed by adding serial dilutions of free PEG (OH-PEG_{3K}-NH_2 and CH_3-

DOI: 10.1021/acs.analchem.7b00730
Anal. Chem. 2017, 89, 6082−6090

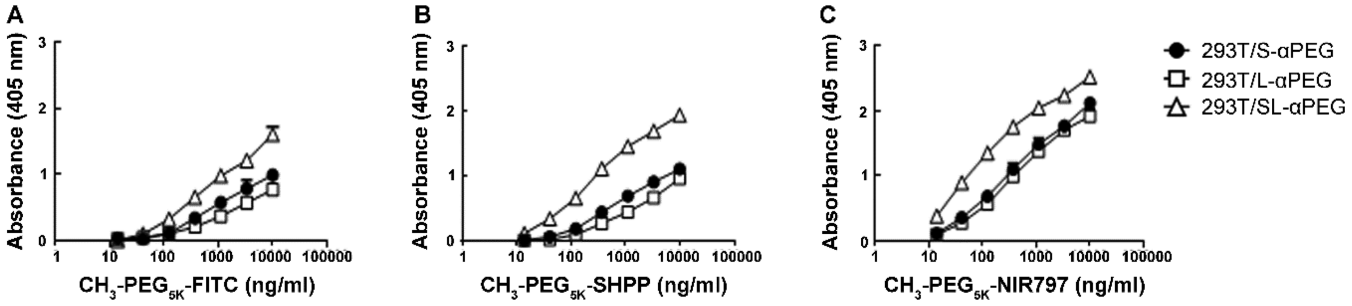

Figure 5. Quantitative cell-based ELISA for PEG-like molecules. Sandwich ELISAs with 293T/SL-αPEG (△), 293T/S-αPEG (●), and 293T/L-αPEG (□) cells as the capture reagents and the biotinylated anti-PEG antibody (AGP4) as the detection antibody were used to measure the concentration of (A) CH_3-PEG_{5K}-FITC, (B) CH_3-PEG_{5K}-SHPP, or (C) CH_3-PEG_{5K}-NIR797. The mean absorbance values (405 nm) of triplicate determinations are shown. The bars indicate the SD.

PEG_{5K}-NH_2) and PEG-like (CH_3-PEG_{5K}-FITC, CH_3-PEG_{5K}-SHPP, and CH_3-PEG_{5K}-NIR797) molecules. Captured molecules were then quantified by sequential addition of biotinylated AGP4 anti-PEG antibody, HRP-conjugated streptavidin, and ABTS substrate. Figures 4 and 5 show that the binding capacities of 293T/SL-αPEG cells for different lengths of free PEG molecules and all three PEG-like molecules were significantly enhanced compared with those of 293T/S-αPEG and 293T/L-αPEG cells. The HRP signal could be amplified by 1.2−183-fold at concentrations ranging from 41 to 10000 ng mL^{-1} free PEG and PEG-like molecules. 293T/SL-αPEG cells could sensitively detect free PEG molecules at a concentration of 41 ng mL^{-1} and PEG-like molecules at concentrations ranging from 14 to 137 ng mL^{-1}, whereas 293T/S-αPEG and 293T/L-αPEG cells showed poor detection ability at the same concentrations. The poor detection ability of uniform-length anti-PEG Fab-expressing cells may be caused by the release of fewer epitopes of PEG molecules after binding to captured antibody than hybrid-type cells, thereby decreasing the binding of detective antibodies and signal amplification (Figure 7). Taken together, these results indicate that the hybrid-type anti-PEG Fab-expressing cells (293T/SL-αPEG cells) provided higher a binding capacity and detection limit for free PEG and PEG-like molecules.

Limited sensitivity is the major stumbling block in traditional quantitative methods for quantifying PEG small molecules. High-performance liquid chromatography (HPLC), especially HPLC coupled with tandem mass spectrometry (HPLC/MS/MS), is a powerful analytical technique that is widely used for the analysis of PEG and PEGylated small drugs.[1] However, multiple pretreatment steps are required to reduce the clinical sample complexity before analysis, and the low tolerance to contamination from surrogate peptides and other truncated metabolite species present in clinical samples restricts its application.[32,33] Radiolabeling offers a highly sensitive method to determine the pharmacokinetics of PEG and PEGylated compounds, but incorporation of radioisotopes may alter the pharmacokinetic properties of small molecules.[34] Methoxy-PEG (mPEG), which is most commonly used for PEG modification due to its minimized cross-linking possibility, is difficult to directly label by radioisotopes.[1] Safety and disposal issues related to radioisotopes, and the sophisticated equipment used, also limit its universality.[1] Although anti-PEG Ab-based ELISA and anti-PEG cell-based sandwich ELISA could specifically and sensitively detect PEGylated proteins and PEGylated nanoparticles in biological fluid, they still suffered from low sensitivity for quantification of free PEG and PEG-like molecules.[22] Our results show that the hybrid-type anti-PEG antibody-expressing 293T cells (293T/SL-αPEG cells) can significantly increase the PEG small-molecule detection limit and binding capacity in comparison with uniform-length anti-PEG antibody-expressing cells (293T/S-αPEG and 293T/L-αPEG cells). We believe that the steric space created by hybrid-lengthsurface anti-PEG antibody-expressing cells can more efficiently and sensitively analyze the pharmacokinetics of PEG small molecular drugs.

Enhancement of the topological space for antigen−antibody interactions can improve the binding capacity and detection limit of cell-based sandwich ELISA. Brown and colleagues showed that immunoglobulin (Ig) projecting from an antigen molecule adsorbed to a microtiter well surface is more accessible for further interactions with a labeled probe and exhibited a 3−5-fold increase in binding capacity as compared to Ig directly bound to the well surface, suggesting that steric effects may be important in determining the detection limit of ELISA.[35] Sakhnini et al. demonstrated that a Fab fragment immobilized via aldehyde functional groups on a resin with smaller pores, i.e., larger surface area, provided a 9-fold increase in $DBC_{100\%}$ (dynamic binding capacity at 100% breakthrough) relative to monoclonal antibody immobilized on CNBr-activated Sepharose beads.[36] Kumada and colleagues also found that coating antibodies in the same orientation on a PS microwell plate could increase the surface area for antigen−antibody interactions and elevate the detection limit in comparison with randomly orientated capture antibodies in traditional ELISA.[21] In our study, we demonstrated that anchoring anti-PEG Fab fragments with a combination of tether lengths on 293T cells (293T/SL-αPEG cells) could significantly increase the binding capacity of CH_3-PEG_{5K}-FITC and eight-arm PEG_{20K}-FITC probes and produce a higher detection limit of free PEG molecules, PEG-like molecules, and PEGylated macromolecules compared to those of uniform-length anti-PEG Fab-expressing cells (293T/S-αPEG and 293T/L-αPEG cells) in cell-based sandwich ELISA. The higher capacity and detection limit of 293T/SL-αPEG cells may result from increasing the loading of PEG molecules and releasing more epitopes for the detective antibody in cell-based sandwich ELISA (Figure 7). The concept of enhancing the topological space of antigen−antibody interactions may be useful for other antibodies and biomaterials. We believe that the unidirectional organization (outward organization) and variable topology of anti-PEG antibodies on the cell surface can bind more repeating epitopes on PEG to improve the binding capacity and sensitive detection of free PEG and PEGylated molecules.

DOI: 10.1021/acs.analchem.7b00730
Anal. Chem. 2017, 89, 6082−6090

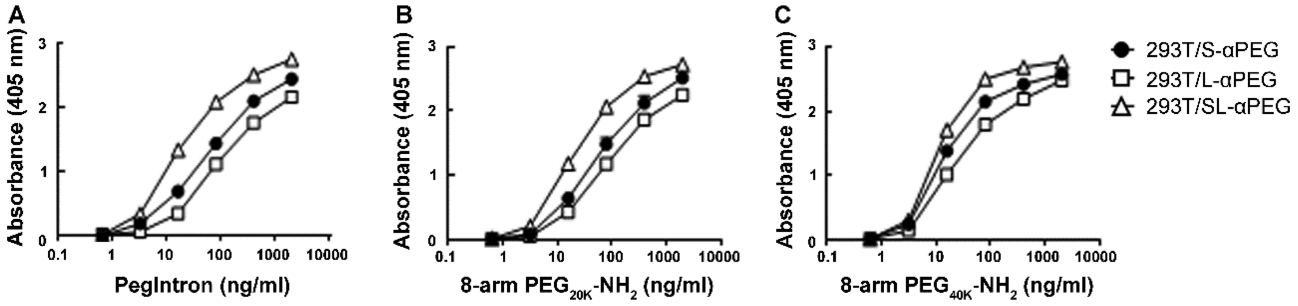

Figure 6. Quantitative cell-based ELISA for macromolecules. Sandwich ELISAs with 293T/SL-αPEG (△), 293T/S-αPEG (●), and 293T/L-αPEG (□) as the capture reagents and biotinylated anti-PEG antibody (AGP4) as the detection antibody to measure the concentration of (A) PegIntron, (B) eight-arm PEG_{20K}-NH_2, or (C) eight-arm PEG_{40K}-NH_2. The mean absorbance values (405 nm) of triplicate determinations are shown. The bars indicate the SD.

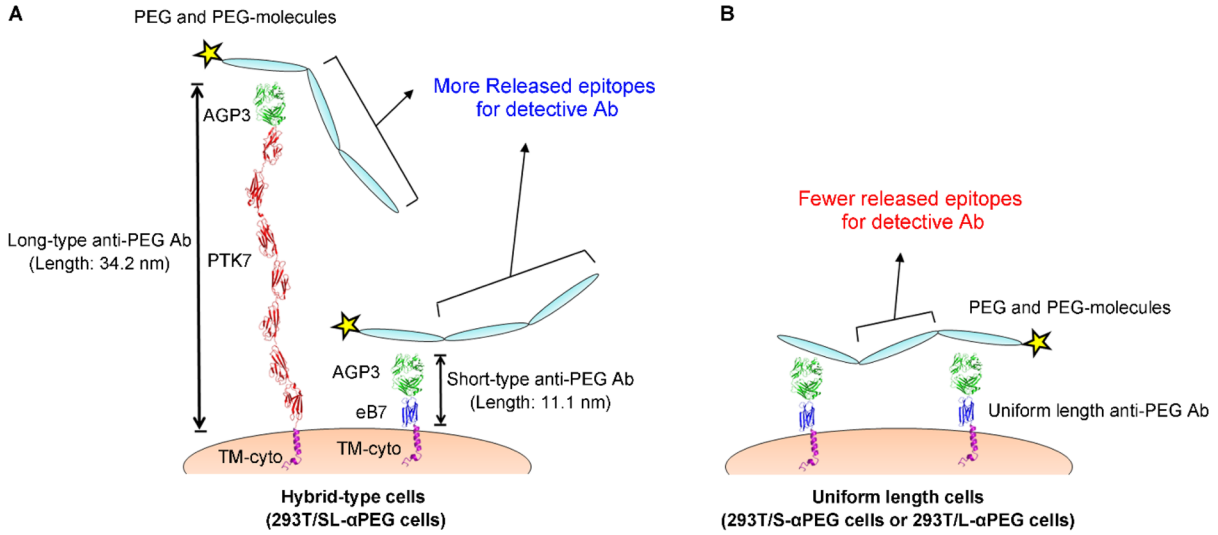

Figure 7. Structure model of short- and long-type anti-PEG antibodies for PEG molecule binding. The structures of the short-type (AGP3-eB7) and long-type (AGP3-PTK7) anti-PEG antibodies were predicted by SWISS modeling. The length of each domain was calculated by PyMol software. (A) Hybrid-type cells (293T/SL-αPEG cells). (B) Uniform-length anti-PEG antibody-expressing cells (293T/S-αPEG and 293T/L-αPEG cells). The anti-PEG Fab (AGP3), seven Ig-like C2 domains of PTK7 (PTK7), Ig-like C2 domain of eB7 (eB7), and transmembrane−cytoplasmic domain (TM−cyto) are shown in green, red, blue, and purple, respectively. The lengths of AGP3 Fab, PTK7, and eB7 were 6.8, 27.4, and 4.3 nm, respectively. Ab = antibody.

Quantification of PEGylated Protein and Multiarm PEG Macromolecules by Anti-PEG Cell-Based Sandwich ELISA. We also analyzed the detection limit of 293T/SL-αPEG (hybrid-type), 293T/S-αPEG (short-type), and 293T/L-αPEG (long-type) cells for a PEGylated protein (CH_3-PEG_{12K}-IFNα-2b; PegIntron) and multiarm PEG macromolecules (eight-arm PEG_{20K}-NH_2 and eight-arm PEG_{40K}-NH_2) using a previously described procedure. As shown in Figure 6, the detection limits of 293T/SL-αPEG cells for quantifying PegIntron, eight-arm PEG_{20K}-NH_2, and eight-arm PEG_{40K}-NH_2 were as low as 3.2−16 ng mL^{-1}. More sensitive detection compared to that for measurement of free PEG molecules is attributed to more binding epitopes on the long PEG molecules on PegIntron and the multiarm PEG molecules. The binding capacity of 293T/SL-αPEG cells was significantly improved at high concentrations (in the range from 16 to 2000 ng mL^{-1}) of PEGylated proteins ($P < 0.001$) and multiarm PEG macromolecules (eight-arm PEG_{20K}-NH_2 and eight-arm PEG_{40K}-NH_2; $P < 0.05$−0.001) compared with that of 293T/S-αPEG and 293T/L-αPEG cells. Together, these results suggest that the 293T/SL-αPEG cells possess a larger binding capacity for detecting PEGylated protein and multiarm PEG molecules in comparison to cells expressing uniform-length anti-PEG antibodies.

Development of a universal tool for the quantification of PEG and PEGylated molecules is desirable. PEG is a water-soluble, nontoxic, low-immunogenicity, biocompatible polymer that has been approved by the FDA for human intravenous, oral, and dermal applications.[1] PEG with various molecular weights has been widely used in biopharmaceuticals. For example, poly(ethylene glycol) 3350 (PEG-3350) is the major component of laxatives (e.g., TriLyte or MiraLax) for treating constipation,[37] methoxy PEG-2K ($mPEG_{2K}$) covalently conjugated on zidovudine (AZT) is used to treat acquired immune deficiency syndrome (AIDS),[38] $mPEG_{2K}$ is also used for liposomal doxorubicin modification (Lipo-Dox) for treatment of several types of cancer,[15] and $mPEG_{30K}$ conjugated to epoetin β (Mircera) is used for treating anemia.[7] Thus, it is important to develop a universal tool for the quantification of different lengths of PEG and PEGylated molecules. Our results show that all of the hybrid-type (293T/SL-αPEG), short-type (293T/S-αPEG) ,and long-type (293T/L-αPEG) cells could sensitively quantify free PEG molecules, PEG-like molecules, and PEGylated macromolecules. Notably, the hybrid-type 293T

DOI: 10.1021/acs.analchem.7b00730
Anal. Chem. 2017, 89, 6082−6090

cells (293T/SL-αPEG cells) displayed the highest binding capacity and sensitivity for quantifying free PEG and PEGylated molecules in a cell-based sandwich ELISA. We think that this universal quantitative tool can properly quantify different lengths of PEG molecules and accelerate the development of PEGylated drugs in research laboratories and in industry.

It is important to develop a low-cost and convenient method for quantitative measurement of PEG and PEGylated drugs during drug development. In traditional ELISA, a high purity of capture antibodies is needed for sample detection. The complex process of antibody purification may add cost and time and even damage the structure of the antibodies, and further affect the antibody's ability to bind to the target antigen. On the other hand, endogenous proteins or clotting factors in serum can also affect the accuracy of traditional quantitative ELISA.[39−41] To avoid a similar situation and simplify the manufacturing process of the drug quantitative ELISA, we generated the anti-PEG antibody-expressing 293T cells (293T/SL-αPEG cells) as a PEG capture reagent. The 293T/SL-αPEG cells can continuously provide a stable and high-quality source of PEG capture cells without requiring additional purification of PEG capture antibodies. We previously showed that skim milk or serum not only did not interfere with the assay detection limit but also greatly enhanced the detection limit of the assay for PEG and PEGylated molecules in the anti-PEG cell-based sandwich ELISA.[22,29,42] Additionally, we also optimized the binding capacity of PEG and PEGylated molecules in 293T/SL-αPEG cells by adjusting the ratio of short-type (AGP3-eB7) and long-type (AGP3-PTK7) anti-PEG antibodies on the cell surface. Unfortunately, the lack of a well-established production line limits the wide usage and/or commercialization of cell-based sandwich ELISA kits in the current market. We expect that the optimized hybrid-type anti-PEG antibody-expressing cells will provide a lower cost, convenient, and sensitive tool for monitoring PEGylated drugs in clinical samples.

Speculative Model for a Higher Capacity and Detection Limit of PEG Molecules in Hybrid-Tethered Anti-PEG Antibody-Expressing 293T Cells. To attempt to explain why the capacity of PEG molecules can be elevated on hybrid-type anti-PEG cells (293T/SL-αPEG cells), we predicted the three-dimensional structure of short-type (AGP3-eB7) and long-type (AGP3-PTK7) anti-PEG Fab with an automated protein structure homology-modeling server, SWISS-Modeling, and calculated the molecular length of each domain by PyMol software (DeLano Scientific). We took PEG_{5K} as an example and assumed an average PEG_{5K} chain length of 5 nm on the basis of the commonly reported value of about 5 nm by Cauda,[43] Cruje,[44] and Xing.[45] The predictive lengths of AGP3-eB7 and AGP3-PTK7 were 11.1 and 34.2 nm, respectively. As shown in Figure 7, binding of the PEG molecules (e.g., PEG_{5K}) to anti-PEG Fab on 293T/SL-αPEG cells may lead to the resident length of PEG out of the AGP3-binding epitope (at least 34 additional OCH_2CH_2 subunits[46]) not being long enough for nearby anti-PEG antibody binding, thereby increasing the binding capacity of 293T/SL-αPEG cells. In addition, the quantitative sensitivity of free PEG and PEGylated molecules in anti-PEG cell-based sandwich ELISA can also be improved by releasing more free epitopes of PEG molecules for the detective antibody (Figure 7A). In contrast, there were few epitopes released from PEG molecules bound on uniform-length anti-PEG antibody-tethered cells (293T/S-αPEG and 293T/L-αPEG cells) due to the fact that one PEG molecule may occupy many antigen-binding sites of anti-PEG antibodies on the cell membrane (Figure 7B). The predictive results indicate that the variable topology created by tethering different lengths of anti-PEG antibodies on the cell membrane may increase the loading and release more epitopes of free PEG and PEGylated molecules for sensitive detection.

CONCLUSIONS

In summary, we demonstrated that varying the topology of anti-PEG antibodies on 293T cells (293T/SL-αPEG cells) allows a higher binding capacity and detection limit for free PEG and PEGylated molecules compared with that of uniform-length anti-PEG antibody-expressing cells (293T/S-αPEG and 293T/L-αPEG cells) in a cell-based sandwich ELISA system. We suggest that this hybrid-length anti-PEG Fab-expressing cell-based sandwich ELISA has the following advantages and potential: (1) more sensitive quantification of PEG and PEGylated molecules; (2) single cloned and membrane anti-PEG Fab highly expressing 293T cells that can continuously provide a stable and high-quality source of PEG capture cells for high-throughput measurement of samples; (3) optimization of the binding capacity of PEGylated molecules in 293T/SL-αPEG cells by adjusting the ratio of short-type (AGP3-eB7) and long-type (AGP3-PTK7) anti-PEG antibodies on the cell surface; (4) potential application of the concept of increasing binding capacity by enhancing the surface area for ligand−receptor interactions in other research fields (e.g., protein purification); (5) potential wide-range use for quantification of PEG-like and PEGylated molecules and consequent acceleration of the process of drug development. We believe that the hybrid-length anti-PEG Fab cell-based sandwich ELISA provides a sensitive, convenient, and universal method that may be used in basic research laboratories and pharmaceutical companies to study the pharmacokinetics of PEG and PEGylated molecules.

AUTHOR INFORMATION

Corresponding Authors

*Phone: +886 7 2911101 8904. Fax: +886 7 2911590. E-mail: fchen@cc.kmu.edu.tw.

*Phone: +886 7 3121101 2697. Fax: +886 7 3227508. E-mail: tlcheng@kmu.edu.tw.

ORCID

Tian-Lu Cheng: 0000-0001-6424-4731

Author Contributions

W.-W.L. and Y.-A.C. contributed equally to this work. F.-M.C. and T.-L.C. designed the research, W.-W.L., Y.-A.C, and B.-M.C, performed the research, W.-W.L., Y.-C.H., S.R.R., F.-M.C., T.-L.C., and Y.-A.C. analyzed and interpreted the data, W.-W.L. wrote the paper; C.-H.K., Y.-C.L., I.-J.C., B.-C.H., Y.-C.T., M.-Y.H., and Y.-T.W. assisted in eliminating problems during the experiments and provided suggestions and corrections for the manuscript.

Notes

The authors declare no competing financial interest.

ACKNOWLEDGMENTS

This work was supported by grants from the National Research Program for Biopharmaceuticals, Ministry of Science and Technology, Taipei, Taiwan (MOST 105-2325-B-037-002, MOST 105-2325-B-037-001, MOST 105-2325-B-041-001, and MOST 105-2314-B-037-010-MY3) and Kaohsiung Medical University (KMU-DK106002 and D08-00005) and KMU Aim

DOI: 10.1021/acs.analchem.7b00730
Anal. Chem. 2017, 89, 6082−6090

for the Top 500 Universities Grants (KMU-TP105C00 and KMU-DT106003). This study was also supported partially by the Grant of Biosignature in Colorectal Cancers, Academia Sinica, Taiwan (BM10501010045), a grant from the Program for Translational Innovation of Biopharmaceutical Development-Technology Supporting Platform Axis, Academia Sinica, Taiwan (GRC106TSPA01), and a grant from the Health and Welfare Surcharge of Tobacco Products (MOHW106-TDU-B-212-144007).

REFERENCES

(1) Cheng, T. L.; Chuang, K. H.; Chen, B. M.; Roffler, S. R. *Bioconjugate Chem.* **2012**, *23*, 881−899.
(2) Rowinsky, E. K.; Rizzo, J.; Ochoa, L.; Takimoto, C. H.; Forouzesh, B.; Schwartz, G.; Hammond, L. A.; Patnaik, A.; Kwiatek, J.; Goetz, A.; Denis, L.; McGuire, J.; Tolcher, A. W. *J. Clin. Oncol.* **2003**, *21*, 148−157.
(3) Mattern, M. R.; Hofmann, G. A.; Polsky, R. M.; Funk, L. R.; McCabe, F. L.; Johnson, R. K. *Oncol Res.* **1993**, *5*, 467−474.
(4) Zhao, H.; Rubio, B.; Sapra, P.; Wu, D. C.; Reddy, P.; Sai, P.; Martinez, A.; Gao, Y.; Lozanguiez, Y.; Longley, C.; Greenberger, L. M.; Horak, I. D. *Bioconjugate Chem.* **2008**, *19*, 849−859.
(5) Greenwald, R. B.; Gilbert, C. W.; Pendri, A.; Conover, C. D.; Xia, J.; Martinez, A. *J. Med. Chem.* **1996**, *39*, 424−431.
(6) Pasut, G.; Veronese, F. M. *J. Controlled Release* **2012**, *161*, 461−472.
(7) Sanchez-Fructuoso, A.; Guirado, L.; Ruiz, J. C.; Torregrosa, V.; Gonzalez, E.; Suarez, M. L.; Gallego, R.; AnemiaTrans Study Group. *Transplant. Proc.* **2010**, *42*, 2931−293410.1016/j.transproceed.2010.09.012.
(8) Manns, M. P.; McHutchison, J. G.; Gordon, S. C.; Rustgi, V. K.; Shiffman, M.; Reindollar, R.; Goodman, Z. D.; Koury, K.; Ling, M.; Albrecht, J. K. *Lancet* **2001**, *358*, 958−965.
(9) Heathcote, E. J.; Shiffman, M. L.; Cooksley, W. G.; Dusheiko, G. M.; Lee, S. S.; Balart, L.; Reindollar, R.; Reddy, R. K.; Wright, T. L.; Lin, A.; Hoffman, J.; De Pamphilis, J. *N. Engl. J. Med.* **2000**, *343*, 1673−1680.
(10) Reddy, K. R.; Wright, T. L.; Pockros, P. J.; Shiffman, M.; Everson, G.; Reindollar, R.; Fried, M. W.; Purdum, P. P., 3rd; Jensen, D.; Smith, C.; Lee, W. M.; Boyer, T. D.; Lin, A.; Pedder, S.; DePamphilis, J. *Hepatology* **2001**, *33*, 433−438.
(11) Molineux, G. *Curr. Pharm. Des.* **2004**, *10*, 1235−1244.
(12) Wang, J.; Fang, X.; Liang, W. *ACS Nano* **2012**, *6*, 5018−5030.
(13) Wang, Q.; Jiang, H.; Li, Y.; Chen, W.; Li, H.; Peng, K.; Zhang, Z.; Sun, X. *Biomaterials* **2017**, *122*, 10−22.
(14) Tang, S.; Meng, Q.; Sun, H.; Su, J.; Yin, Q.; Zhang, Z.; Yu, H.; Chen, L.; Gu, W.; Li, Y. *Biomaterials* **2017**, *114*, 44−53.
(15) Barenholz, Y. *J. Controlled Release* **2012**, *160*, 117−134.
(16) Stefanick, J. F.; Ashley, J. D.; Kiziltepe, T.; Bilgicer, B. *ACS Nano* **2013**, *7*, 2935−2947.
(17) Passero, F. C., Jr.; Grapsa, D.; Syrigos, K. N.; Saif, M. W. *Expert Rev. Anticancer Ther.* **2016**, *16*, 697−703.
(18) Rammohan, A.; Mishra, G.; Mahaling, B.; Tayal, L.; Mukhopadhyay, A.; Gambhir, S.; Sharma, A.; Sivakumar, S. *ACS Appl. Mater. Interfaces* **2016**, *8*, 350−362.
(19) Hu, Y.; Haynes, M. T.; Wang, Y.; Liu, F.; Huang, L. *ACS Nano* **2013**, *7*, 5376−5384.
(20) Nance, E.; Zhang, C.; Shih, T. Y.; Xu, Q.; Schuster, B. S.; Hanes, J. *ACS Nano* **2014**, *8*, 10655−10664.
(21) Kumada, Y.; Hamasaki, K.; Shiritani, Y.; Ohse, T.; Kishimoto, M. *J. Biotechnol.* **2009**, *142*, 135−141.
(22) Chuang, K. H.; Tzou, S. C.; Cheng, T. C.; Kao, C. H.; Tseng, W. L.; Shiea, J.; Liao, K. W.; Wang, Y. M.; Chang, Y. C.; Huang, B. J.; Wu, C. J.; Chu, P. Y.; Roffler, S. R.; Cheng, T. L. *Anal. Chem.* **2010**, *82*, 2355−2362.
(23) Jain, P.; Vyas, M. K.; Geiger, J. H.; Baker, G. L.; Bruening, M. L. *Biomacromolecules* **2010**, *11*, 1019−1026.
(24) Barua, S.; Yoo, J. W.; Kolhar, P.; Wakankar, A.; Gokarn, Y. R.; Mitragotri, S. *Proc. Natl. Acad. Sci. U. S. A.* **2013**, *110*, 3270−3275.
(25) Chuang, K. H.; Wang, H. E.; Cheng, T. C.; Tzou, S. C.; Tseng, W. L.; Hung, W. C.; Tai, M. H.; Chang, T. K.; Roffler, S. R.; Cheng, T. L. *J. Nucl. Med.* **2010**, *51*, 933−941.
(26) Tsai, N. M.; Cheng, T. L.; Roffler, S. R. *Biotechniques* **2001**, *30*, 396−402.
(27) Roffler, S. R.; Wang, H. E.; Yu, H. M.; Chang, W. D.; Cheng, C. M.; Lu, Y. L.; Chen, B. M.; Cheng, T. L. *Gene Ther.* **2006**, *13*, 412−420.
(28) Fang, J.; Qian, J. J.; Yi, S.; Harding, T. C.; Tu, G. H.; VanRoey, M.; Jooss, K. *Nat. Biotechnol.* **2005**, *23*, 584−590.
(29) Hsieh, Y. C.; Cheng, T. C.; Wang, H. E.; Li, J. J.; Lin, W. W.; Huang, C. C.; Chuang, C. H.; Wang, Y. T.; Wang, J. Y.; Roffler, S. R.; Chuang, K. H.; Cheng, T. L. *Sci. Rep.* **2016**, *6*, 39119.
(30) Tyler, B.; Gullotti, D.; Mangraviti, A.; Utsuki, T.; Brem, H. *Adv. Drug Delivery Rev.* **2016**, *107*, 163−175.
(31) Bhavsar, M. D.; Amiji, M. M. *AAPS PharmSciTech* **2008**, *9*, 288−294.
(32) Novakova, L.; Vlckova, H. *Anal. Chim. Acta* **2009**, *656*, 8−35.
(33) Xu, Y.; Mehl, J. T.; Bakhtiar, R.; Woolf, E. J. *Anal. Chem.* **2010**, *82*, 6877−6886.
(34) Seo, J. W.; Zhang, H.; Kukis, D. L.; Meares, C. F.; Ferrara, K. W. *Bioconjugate Chem.* **2008**, *19*, 2577−2584.
(35) Brown, D. W.; Kim, Y. T.; Siskind, G. W. *J. Immunol. Methods* **1989**, *116*, 45−51.
(36) Sakhnini, L. I.; Pedersen, A. K.; Ahmadian, H.; Hansen, J. J.; Bulow, L.; Dainiak, M. *Journal of chromatography. A* **2016**, *1468*, 143−153.
(37) Phatak, U. P.; Pashankar, D. S. *Clin. Pediatr. (Philadelphia)* **2014**, *53*, 927−932.
(38) Li, W.; Chang, Y.; Zhan, P.; Zhang, N.; Liu, X.; Pannecouque, C.; De Clercq, E. *ChemMedChem* **2010**, *5*, 1893−1898.
(39) Nielsen, K.; Kelly, L.; Gall, D.; Smith, P.; Bosse, J.; Nicoletti, P.; Kelly, W. *Vet. Res. Commun.* **1994**, *18*, 433−437.
(40) Urbonaviciute, V.; Furnrohr, B. G.; Weber, C.; Haslbeck, M.; Wilhelm, S.; Herrmann, M.; Voll, R. E. *J. Leukocyte Biol.* **2007**, *81*, 67−74.
(41) DeForge, L. E.; Shih, D. H.; Kennedy, D.; Totpal, K.; Chuntharapai, A.; Bennett, G. L.; Drummond, J. H.; Siguenza, P.; Wong, W. L. *J. Immunol. Methods* **2007**, *320*, 58−69.
(42) Chuang, K. H.; Kao, C. H.; Roffler, S. R.; Lu, S. J.; Cheng, T. C.; Wang, Y. M.; Chuang, C. H.; Hsieh, Y. C.; Wang, Y. T.; Wang, J. Y.; Weng, K. Y.; Cheng, T. L. *Macromolecules* **2014**, *47*, 6880−6888.
(43) Cauda, V.; Argyo, C.; Bein, T. *J. Mater. Chem.* **2010**, *20*, 8693−8699.
(44) Cruje, C.; Chithrani, D. B. *J. Nanomed Res.* **2014**, *1*, 00006.
(45) Xing, H.; Li, J.; Xu, W.; Hwang, K.; Wu, P.; Yin, Q.; Li, Z.; Cheng, J.; Lu, Y. *ChemBioChem* **2016**, *17*, 1111−1117.
(46) Cheng, T. L.; Cheng, C. M.; Chen, B. M.; Tsao, D. A.; Chuang, K. H.; Hsiao, S. W.; Lin, Y. H.; Roffler, S. R. *Bioconjugate Chem.* **2005**, *16*, 1225−1231.

DOI: 10.1021/acs.analchem.7b00730
Anal. Chem. 2017, 89, 6082−6090